 CMES, vol.63, no.3, pp.243-263, 2010

On Increasing Computational Efficiency of Local Integral Equation Method Combined with Meshless Implementations

V. Sladek[1], **J. Sladek**[1] **and Ch. Zhang**[2]

Abstract: The paper deals with diminishing the prolongation of the computational time due to procedural evaluation of the shape functions and their derivatives in weak formulations implemented with meshless approximations. The proposed numerical techniques are applied to problems of stationary heat conduction in functionally graded media. Besides the investigation of the computational efficiency also the accuracy and convergence study are performed in numerical tests.

Keywords: strong and weak formulations, Moving Least Squares approximation, computational time, accuracy, convergence, potential problem

1 Introduction

In two last decades, mesh-free methods have become popular and well developed in various branches of science and engineering. Practically it is impossible to give a comprehensive review of the literature devoted to the development and applications of mesh-free methods. It is neither the aim of this paper to refer the most recent works in that field. Instead of this, we mention three journals (CMES-Computer Modeling in Engineering & Sciences, EABE-Engineering Analysis with Boundary Elements, IJNME-International Journal for Numerical Methods in Engineering) publishing plenty of contributions to mesh-free simulations of engineering problems. The application of the weak formulation on local sub-domains enables development of truly mesh-free formulations in contrast to the weak formulations considered in the global sense, where the background mesh is still required (Atluri et al (2003), Atluri (2004)). Besides the numerous advantages of mesh-free methods (simple pre-processing, elimination of re-meshing, numerical stability in large dis-

[1] Institute of Construction and Architecture, Slovak Academy of Sciences, 845 03 Bratislava, Slovakia (vladimir.sladek@savba.sk, jan.sladek@savba.sk)

[2] Department of Civil Engineering, University of Siegen, Paul-Bonatz-Str. 9-11, D-57076 Siegen, Germany (c.zhang@uni-siegen.de)

tortions, efficient modeling of separable media, etc), there is one handicap consisting in prolongation of the computational time which is due to procedural evaluation of shape functions in contrast to polynomial shape functions utilized in mesh-based methods.

In this paper, we propose several improvements upon the application of the standard Moving Least Squares (MLS) approximation (Atluri (2004), Lancaster and Salkauskas (1981)) to mesh-free formulations for solution of boundary value problems. Apparently the prolongation of the computational time is increasing with increasing the amount of points at which the shape functions are required. Therefore the strong formulations with collocating the governing partial differential equations only at nodal points guarantee better computational economy than the weak formulations with integrating over the analyzed domain or at least over its boundary. On the other hand in strong formulations, we need higher order derivatives of the field variable whose accuracy is decreasing with increasing the order of differentiation and also the computational complexity is increasing. We shall discuss both the strong and weak formulations. Certain time savings can be achieved by using MLS-CAN (Central Approximation Node) concept (Sladek et al (2008a,b)). Another saving is achieved by performing the integrations in the weak formulation analytically (Sladek et al (2008c), (2009), (2010)). Then, we need the derivatives of the shape functions only at nodal points. However, the order of the derivatives is increased. Besides the standard differentiation we propose also a modified differentiation with improving the accuracy of higher order derivatives. Savings in computational time by new proposed computational techniques are quantified in order to assess the computational economy. The accuracy and convergence study are performed too. All the numerical experimentation is performed on a simple example for the stationary heat conduction in a square domain of functionally graded medium. The analytical solution is employed as the benchmark solution. The computational effort in the proposed weak formulation resembles that in the finite difference method. The relationship with the strong formulation based on the collocation of the partial differential equation at nodal points is discussed too. Consideration of the material non-homogeneity does not give rice to any complication as compared with the homogeneous case.

2 Stationary potential problems. Governing equations.

The governing equation for stationary potential problems in anisotropic and continuously non-homogeneous media is given by the partial differential equation of elliptic type with variable coefficients (Wrobel (2002))

$$\left(\lambda_{ik}(\mathbf{x})u_{,k}(\mathbf{x})\right)_{,i} = -w(\mathbf{x}), \quad \text{in } \Omega \tag{1}$$

where $u(\mathbf{x})$ is the potential field, $w(\mathbf{x})$ is the volume density of sources, and $\lambda_{ik}(\mathbf{x})$ is the tensor of material coefficients (e.g., thermal conductivities). The left-hand side of Eq. (1) is the divergence of the flux vector

$$q_k(\mathbf{x}) = -\lambda_{ik}(\mathbf{x})u_{,i}(\mathbf{x}) \tag{2}$$

The physically reasonable boundary conditions of the problem can be of the following types:

(i) Dirichlet b.c.:

$$u(\boldsymbol{\eta}) = \tilde{u}(\boldsymbol{\eta}) \text{ at } \boldsymbol{\eta} \in \partial\Omega_D,$$

(ii) Neumann b.c.:

$$n_i(\boldsymbol{\eta})q_i(\boldsymbol{\eta}) = \tilde{q}(\boldsymbol{\eta}) \text{ at } \boldsymbol{\eta} \in \partial\Omega_N, \tag{3}$$

(iii) Robin b.c.:

$$\alpha u(\boldsymbol{\eta}) + \beta n_i(\boldsymbol{\eta})q_i(\boldsymbol{\eta}) = 0 \text{ at } \boldsymbol{\eta} \in \partial\Omega_R,$$

where $\partial\Omega = \partial\Omega_D \cup \partial\Omega_N \cup \partial\Omega_R$, $n_i(\boldsymbol{\eta})$ is the unit outward normal vector to the boundary, α and β are real constants, and a tilde over a quantity denotes the prescribed value.

The governing equation in the differential form (1) is derived form the physical balance principles which take an integral form in a continuum theory. Let us consider an arbitrary piece of continuum contained in a domain Ω^c bounded with the boundary $\partial\Omega^c$. Then, the energy balance for a steady state field in the considered piece of continuum is expressed as

$$\int_{\partial\Omega^c} n_i(\boldsymbol{\eta})q_i(\eta)d\Gamma(\boldsymbol{\eta}) = \int_{\Omega^c} w(\mathbf{x})d\Omega(\mathbf{x}) \tag{4}$$

In view of the Gauss divergence theorem, one can see that Eq. (4) is an equivalent of Eq. (1) since each of them can be derived from the other one under the assumption of arbitrary choice of the sub-domain $\Omega^c \subset \Omega$.

3 Strong and local weak formulations

The main difference between the differential and integral forms of the governing equations consists in the order of differentiation. This feature is rather important

from the point of view of numerical implementation, since the accuracy of approximated derivatives is usually decreasing with increasing the order of the differentiation. Another aspect is the effort for the numerical integration and evaluation of the shape functions at integration points.

It is well known that the fundamental solution for the governing PDE with variable coefficients is not available in closed form, in general. Consequently, neither a pure boundary formulation is available, in general. Thus, the discrete unknowns will be associated with nodes distributed in both the analyzed domain and its boundary. On the other hand, utilization of a domain-type approximation (when the dimension of the approximation domain is the same as that of the analyzed domain) enables us to express approximations of derivatives of the field variable by differentiating the approximation of the field variable. Then, the same discrete d.o.f. as used for approximation of both the field variable and its derivatives. Without any detailed specifications, we assume the potential field to be approximated within a sub-domain $\Omega_x \subset \Omega$ in terms of certain nodal values $\hat{u}^a$ and shape functions $\varphi^a(\mathbf{x})$ as

$$u(\mathbf{x}) = \sum_a \hat{u}^a \varphi^a(\mathbf{x}), \tag{5}$$

where the sets of nodes contributing to the summations are dependent on the point of approximation (Liu 2003)). Then, the derivatives of the potential field can be approximated in terms of the same nodal values and the derivatives of the shape functions as

$$u_{,ij\ldots}(\mathbf{x}) = \sum_a \hat{u}^a \varphi^a_{,ij\ldots}(\mathbf{x}) \tag{6}$$

Such an approach will be referred as standard differentiation approach (*sdif*). Now, one can discretize both the governing equations and the boundary conditions. Collocating the boundary conditions at boundary nodes and the governing equation (1) at interior nodes, one obtains the discretized strong formulation

$$\sum_a \hat{u}^a \varphi^a(\boldsymbol{\eta}^b) = \tilde{u}(\boldsymbol{\eta}^b) \text{ at } \boldsymbol{\eta}^b \in \partial\Omega_D \tag{7a}$$

$$-n_i(\boldsymbol{\eta}^b)\lambda_{ik}(\boldsymbol{\eta}^b)\sum_a \hat{u}^a \varphi^a_{,k}(\boldsymbol{\eta}^b) = \tilde{q}(\boldsymbol{\eta}^b) \text{ at } \boldsymbol{\eta}^b \in \partial\Omega_N \tag{7b}$$

$$\sum_a \hat{u}^a \left\{ \alpha\varphi^a(\boldsymbol{\eta}^b) - \beta n_i(\boldsymbol{\eta}^b)\lambda_{ik}(\boldsymbol{\eta}^b)\varphi^a_{,k}(\boldsymbol{\eta}^b) \right\} = 0 \text{ at } \boldsymbol{\eta}^b \in \partial\Omega_R \tag{7c}$$

$$\lambda_{ik}(\mathbf{x}^c)\sum_a u^a \varphi^a_{,ik}(\mathbf{x}^c) + \lambda_{ik,i}(\mathbf{x}^c)\sum_a u^a \varphi^a_{,k}(\mathbf{x}^c) = -w(\mathbf{x}^c) \text{ at } \mathbf{x}^c \in \Omega, \tag{8}$$

Equation (8) will be referred as CPDE – collocated partial differential equation. Alternatively to the strong formulation, one can get the local weak formulation replacing Eq.(8) by the discretized LIE (4)

$$\sum_a u^a \int\limits_{\partial\Omega^c} n_i(\eta)\lambda_{ik}(\boldsymbol{\eta})\varphi^a_{,k}(\boldsymbol{\eta})d\Gamma(\boldsymbol{\eta}) = -\int\limits_{\Omega^c} w(\mathbf{x})d\Omega(\mathbf{x}) \text{ at } \mathbf{x}^c \in \Omega. \tag{9}$$

Strictly speaking, the utilization of Eq.(9) with collocated boundary conditions (7) yields a mixed formulation in which the governing equation is considered in a weak sense while the boundary conditions in the strong sense.

3.1 Analytical integrations in local weak formulation

The main advantage of the weak formulation is the lowest order of the derivative of the field variable. On the other hand, the gradients of the shape functions are to be evaluated at each integration point what is the main handicap of this formulation as long as the shape functions and their derivatives are not available in closed form, but a procedural evaluation is necessary. Therefore our aim is to perform the integrations analytically when the evaluation of the derivatives of the shape functions is reduced to nodal points (Sladek et al (2008c)). For this purpose, we assume circular sub-domains $\partial\Omega^c$ around each interior $\mathbf{x}^c$ node and employ the Taylor series expansion for the gradients of the potential field and the material coefficients

$$u_{,k}(\boldsymbol{\eta})|_{\partial\Omega^c} \doteq u_{,k}(\mathbf{x}^c) + r^c_s n_p(\eta)u_{,kp}(\mathbf{x}^c) + \frac{(r^c_s)^2}{2} n_p(\boldsymbol{\eta})n_s(\boldsymbol{\eta})u_{,kps}(\mathbf{x}^c) + \ldots \tag{10}$$

$$\lambda(\boldsymbol{\eta})|_{\partial\Omega^c} \doteq \lambda(\mathbf{x}^c) + r^c_s n_m(\eta)\lambda_{,m}(\mathbf{x}^c) + \frac{(r^c_s)^2}{2} n_m(\boldsymbol{\eta})n_t(\boldsymbol{\eta})\lambda_{,mt}(\mathbf{x}^c) + \ldots, \tag{11}$$

where r^c_s is the radius of the sub-domain and $n_i(\boldsymbol{\eta})$ is the unit outward normal vector to $\partial\Omega^c$ at $\boldsymbol{\eta}$. For simplicity, we consider the medium with gradation $\lambda_{ik}(\mathbf{x}) = \lambda^o_{ik}\lambda(\mathbf{x})$.

Assuming the Taylor series expansions up to 6^{th} and 4^{th} orders for $\lambda(\mathbf{x})$ and $\phi_{,i}(\mathbf{x})$, respectively, and neglecting the terms $O\left((r^c_s)^8\right)$, one can accomplish the integration on the l.h.s. of Eq. (9) with the result

$$\frac{\lambda^o_{ik}}{\pi(r^c_s)^2} \int\limits_{\partial\Omega^c} n_i(\boldsymbol{\eta})\lambda(\boldsymbol{\eta})u_{,k}(\boldsymbol{\eta})d\Gamma =$$

$$A^c_k u_{,k}(\mathbf{x}^c) + A^c_{kp}u_{,kp}(\mathbf{x}^c) + A^c_{kps}u_{,kps}(\mathbf{x}^c) + A^c_{kptf}u_{,kptf}(\mathbf{x}^c)$$

and Eq. (9) is converted into the truncated LIE(ai)

$$A^c_k u_{,k}(\mathbf{x}^c) + A^c_{kp} u_{,kp}(\mathbf{x}^c) + A^c_{kps} u_{,kps}(\mathbf{x}^c) + A^c_{kptf} u_{,kptf}(\mathbf{x}^c) = - \frac{1}{\pi (r^c_s)^2} \int_{\Omega^c} w(\mathbf{x}) d\Omega(\mathbf{x}), \quad (12)$$

with

$$A^c_k = \lambda^o_{ik} \left(\lambda^c_{,i} + \frac{(r^c_s)^2}{8} \lambda^c_{,imm} + \frac{(r^c_s)^4}{24} \frac{1}{8} \lambda^c_{,immss} \right)$$

$$A^c_{kp} = \lambda^o_{ik} \left[\lambda^c \delta_{ip} + \frac{(r^c_s)^2}{8} \left(2\lambda^c_{,ip} + \lambda^c_{,jj} \delta_{ip} \right) + \frac{(r^c_s)^4}{24} \left(\frac{1}{2} \lambda^c_{,ipjj} + \frac{\delta_{ip}}{8} \lambda^c_{,ssjj} \right) + \frac{(r^c_s)^6}{256} \left(\frac{1}{6} \lambda^c_{,ipjjss} + \frac{\delta_{ip}}{36} \lambda^c_{,ssjjll} \right) \right]$$

$$A^c_{kps} = \lambda^o_{ik} \left[\frac{(r^c_s)^2}{8} 3\lambda^c_{,i} \delta_{ps} + \frac{(r^c_s)^4}{24} \left(\frac{3}{4} \lambda^c_{,ijj} \delta_{ps} + \frac{1}{2} \lambda^c_{,ips} \right) + \frac{(r^c_s)^6}{256} \left(\frac{1}{4} \lambda^c_{,ijjll} \delta_{ps} + \frac{1}{3} \lambda^c_{,ispjj} \right) \right]$$

$$A^c_{kptf} = \lambda^o_{ik} \left[\frac{(r^c_s)^2}{8} \lambda^c \delta_{ip} \delta_{tf} + \frac{(r^c_s)^4}{24} \left(\lambda^c_{,ip} \delta_{tf} + \frac{1}{4} \lambda^c_{,jj} \delta_{ip} \delta_{tf} \right) + \frac{(r^c_s)^6}{6 \times 24 \times 192} \left(72\lambda^c_{,ipjj} \delta_{tf} + 24\lambda^c_{,iptf} + 9\lambda^c_{,jjll} \delta_{ip} \delta_{tf} \right) \right]$$

In the derivation of Eq. (12), we have utilized the following integrals

$$\frac{1}{r^c_s} \int_{\partial\Omega^c} n_i n_j d\Gamma = \int_0^{2\pi} n_i n_j d\varphi = \pi \delta_{ij},$$

$$\int_0^{2\pi} n_i n_j n_m n_p d\varphi = \frac{\pi}{4} \left(\delta_{ij} \delta_{mp} + \delta_{im} \delta_{jp} + \delta_{ip} \delta_{jm} \right) \equiv \frac{\pi}{4} Y_{ijmp},$$

$$\int_0^{2\pi} n_i n_j n_m n_p n_t n_s d\varphi = \frac{\pi}{24}\left(\delta_{ij}Y_{mpts} + \delta_{im}Y_{jpts} + \delta_{ip}Y_{jmts} + \delta_{it}Y_{jmps} + \delta_{is}Y_{jmpt}\right) \equiv \frac{\pi}{24}Y_{ijmpts},$$

$$\int_0^{2\pi} n_i n_j n_m n_p n_t n_s n_r n_l d\varphi = \frac{\pi}{192}\left(\delta_{ij}Y_{mptsrl} + \delta_{im}Y_{jptsrl} + \delta_{ip}Y_{jmtsrl} + \delta_{it}Y_{jmpsrl} + \delta_{is}Y_{jmptrl} + \delta_{ir}Y_{jmptsl} + \delta_{il}Y_{jmptsr}\right) \quad (13)$$

and the integrals of the product of odd number of normal vectors are vanishing. In the limit $r_s^c \to 0$, Eq. (12) converges to the equation

$$\lambda_{ik}^o \lambda(\mathbf{x}^c) u_{,ik}(\mathbf{x}^c) + \lambda_{ik}^o \lambda_{,i}(\mathbf{x}^c) u_{,k}(\mathbf{x}^c) = -w(\mathbf{x}^c)$$

or

$$\lambda_{ik}(\mathbf{x}^c) \sum_a \hat{u}^a \varphi_{,ik}^a(\mathbf{x}^c) + \lambda_{ik,i}(\mathbf{x}^c) \sum_a \hat{u}^a \varphi_{,k}^a(\mathbf{x}^c) = -w(\mathbf{x}^c) \quad (14)$$

which is equivalent with Eq. (8) derived from the strong formulation (CPDE). Thus, the strong formulation corresponds to the lowest order expansion terms in the weak formulation when the material coefficients and the shape functions gradients are expanded into Taylor series. Hence, one can expect better accuracy by the weak formulation than by the CPDE approach especially for problems in considerably graded materials. Note that the functional dependence of the material coefficients is usually known and hence also the derivatives of the material coefficients are known. However, the derivatives of the unknown solution for the potential field can be considered only approximately in terms of the derivatives of the shape functions. Bearing in mind the expected inaccuracy for approximations of higher-order derivatives, our aim is to decrease the order of the derivatives used in the Taylor series expansion. Therefore the radius of sub-domains r_s^c should be selected sufficiently small.

4 Moving Least Squares (MLS)-approximation

The MLS-approximation (Lancaster and Salkauskas (1981)) belongs to mesh free approximations since no predefined connectivity among nodal points is required.

Besides the standard MLS-approximation, we shall shortly discuss also the Central Approximation Node (CAN) concept (Sladek et al (2008a,b)) resulting in certain saving in computational time.

4.1 Standard MLS approximation

The primary field variable (potential field) is assumed to be approximated at a vicinity of the point $\mathbf{x}$ as

$$u(\mathbf{x}) \approx \sum_{\mu=1}^{m} p^{\mu}(\mathbf{x}) c^{\mu}(\mathbf{x}), \tag{15}$$

where $\{p_1(\mathbf{x}), ..., p_m(\mathbf{x})\}$ is a complete monomial basis and $c^{\mu}(\mathbf{x})$ are expansion coefficients which can be obtained by minimizing a weighted functional

$$J(\mathbf{x}) = \sum_{a=1}^{N_t} \sum_{\mu=1}^{m} w^a(\mathbf{x}) \left[p^{\mu}(\mathbf{x}^a) c^{\mu}(\mathbf{x}) - \hat{u}^a \right]^2, \tag{16}$$

where N_t is the total number of nodes $\mathbf{x}^a (a = 1, 2, ..., N_t)$ and $w^a(\mathbf{x})$ is the weight function associated with node $\mathbf{x}^a$. Hence, one can get the expansion coefficients and the approximation (15) becomes

$$u(\mathbf{x}) \approx u^h(\mathbf{x}) = \sum_{a=1}^{N_t} \phi^a(\mathbf{x}) \hat{u}^a, \quad \phi^a(\mathbf{x}) = \sum_{\mu,\gamma=1}^{m} p^{\mu}(\mathbf{x}) \left(\mathrm{A}^{-1} \right)^{\mu\gamma}(\mathbf{x}) \mathrm{B}^{\gamma a}(\mathbf{x}), \tag{17a}$$

where

$$\mathrm{A}^{\mu\beta}(\mathbf{x}) = \sum_{a=1}^{N_t} w^a(\mathbf{x}) p^{\mu}(\mathbf{x}^a) p^{\beta}(\mathbf{x}^a), \quad \mathrm{B}^{\gamma a}(\mathbf{x}) = w^a(\mathbf{x}) p^{\gamma}(\mathbf{x}^a). \tag{18}$$

Recall that the shape functions $\phi^a(\mathbf{x})$ are not known in closed form and a computational procedure must run for evaluation at each approximation point $\mathbf{x}$. This is the main handicap of mesh-free approximations as compared with mesh-based approximations utilizing mostly polynomial interpolations. The weight function for each node $\mathbf{x}^a$ is chosen as a function with a compact support given by the radius r^a. In this paper, we shall consider Gaussian weight functions:

$$w^a(\mathbf{x}) = \begin{cases} \left[e^{-(d^a/c^a)^2} - e^{-(r^a/c^a)^2} \right] / \left[1 - e^{-(r^a/c^a)^2} \right] & \text{for } 0 \le d^a \le r^a \\ 0 & \text{for } d^a \ge r^a \end{cases} \tag{19}$$

$d^a = |\mathbf{x} - \mathbf{x}^a|$.

Recall that the nodal points are distributed within the analyzed domain arbitrarily and no connectivity is assumed among the nodal points. The actual number of nodes contributing to the approximation (17a) N_x is less than N_t, since the shape function $\phi^a(\mathbf{x}) = 0$, if $w^a(\mathbf{x}) = 0$. Nevertheless, all the N_t nodes are involved into the evaluation algorithm for the shape functions. The radius r^a should be large enough, in order to have a sufficient number of nodes covered in the domain of definition of every sample point ($N_x \geq m$) to ensure the regularity of the matrix $\mathbf{A}$. Recall that the shape functions do not satisfy the Kronecker delta property $\phi^a(\mathbf{x}^b) \neq \delta_{ab}$, in general, and the expansion coefficients $\hat{u}^a$ are fictitious nodal values (Atluri (2004)). These nodal unknowns are discrete degrees of freedom in the discretized formulation.

4.2 MLS-CAN concept

Let $\mathbf{x}^q$ be the central approximation node for the approximation at a point $\mathbf{x}$. Then, the amount of nodes involved into the approximation at $\mathbf{x}$ is reduced a-priori from N_t to N^q, where N^q is the number of nodes supporting the approximation at the CAN $\mathbf{x}^q$, i.e. the amount of nodes in the set $\mathscr{M}^q = \{\forall \mathbf{x}^a;\ w^a(\mathbf{x}^q) > 0\}_{a=1}^{N_t}$. Then, instead of the approximation given by Eq. (17a), we shall use

$$u(\mathbf{x}) \approx u^h(\mathbf{x}) = \sum_{a=1}^{N^q} \hat{u}^{n(q,a)} \phi^{n(q,a)}(\mathbf{x}), \tag{17b}$$

where $n(q,a)$ is the global number of the a-th local node from $\mathscr{M}^q$. In this paper, we shall specify the CAN $\mathbf{x}^q$ as the nearest node to the approximation point $\mathbf{x}$.

4.3 Approximation of derivatives of the potential field

In view of the standard differentiation approach, the gradients of the potential field can be approximated as gradients of the approximated potential field by

$$u_{,j}(\mathbf{x}) \approx u^h_{,j}(\mathbf{x}) = \sum_{a=1}^{N_t} \hat{u}^a \phi^a_{,j}(\mathbf{x}), \tag{20a}$$

in the standard MLS approach, while in the MLS – CAN approach we have

$$u_{,j}(\mathbf{x}) \approx u^h_{,j}(\mathbf{x}) = \sum_{a=1}^{N^q} \hat{u}^{n(q,a)} \phi^{n(q,a)}_{,j}(\mathbf{x}). \tag{20b}$$

Note that calculation of gradients of the shape functions is rather complex proce-

dure according to the formula

$$\phi^a_{,j}(\mathbf{x}) = \sum_{\mu,\gamma=1}^{m} p^\mu_{,j}(\mathbf{x}) \left(\mathrm{A}^{-1}\right)^{\mu\gamma}(\mathbf{x})\mathrm{B}^{\gamma a}(\mathbf{x}) + \sum_{\mu,\gamma=1}^{m} p^\mu(\mathbf{x}) \left[\left(\mathrm{A}^{-1}\right)^{\mu\gamma}(\mathbf{x})\mathrm{B}^{\gamma a}_{,j}(\mathbf{x}) - \sum_{\beta,\lambda=1}^{m} \left(\mathrm{A}^{-1}\right)^{\mu\beta}(\mathbf{x})\mathrm{A}^{\beta\lambda}(\mathbf{x}) \left(\mathrm{A}^{-1}\right)^{\lambda\gamma}(\mathbf{x})\mathrm{B}^{\gamma a}(\mathbf{x})\right]. \quad (21)$$

The higher order derivatives can be obtained in a similar way as

$$u_{,j\ldots k}(\mathbf{x}) \approx u^h_{,j\ldots k}(\mathbf{x}) = \sum_{a=1}^{N_t} \hat{u}^a \phi^a_{,j\ldots k}(\mathbf{x}) \quad (22a)$$

for the standard MLS approach, and for the MLS-CAN approach as

$$u_{,j\ldots k}(\mathbf{x}) \approx u^h_{,j\ldots k}(\mathbf{x}) = \sum_{a=1}^{N^q} \hat{u}^{n(q,a)} \phi^{n(q,a)}_{,j\ldots k}(\mathbf{x}). \quad (22b)$$

Apparently, higher order derivatives of the shape functions increase the complexity of the evaluation. According to experience we know that the accuracy of higher order derivatives fails. In Sect. 3, we have seen that the 1^{st} order derivatives of the shape functions are required at each integration point in the local weak formulation (LIE + numerical integration), the 1^{st} and 2^{nd} order derivatives at nodal points are needed in the strong formulation (CPDE), while higher-order derivatives at nodal points are required in the weak formulation combined with analytical integration.

Beside the *standard differentiation (sdif)* presented above, we shall use also the *modified differentiation* (*mdif*). In the *mdif* approach (Wen and Aliabadi (2008), Sladek et al (2008c), (2009)), the higher order derivatives of the potential field will be expressed in terms of the first order derivatives of the shape functions $F^{ca}_k = \phi^{n(c,a)}_{,k}(\mathbf{x}^c)$ and the nodal values $\hat{u}^{n(c,a)}$ using the recurrent formula

$$u^{(r)}_{,j\ldots k}(\mathbf{x}^c) \approx \sum_{a=1}^{N^c} u^{(r-1)}_{,j\ldots}(\mathbf{x}^{n(c,a)}) \phi^{n(c,a)}_{,k}(\mathbf{x}^c), \quad (23)$$

where the nodal values of the $(r-1)$ - order derivatives and the first order derivatives of the shape functions are used for approximation of the r-order derivative of the potential at nodal points with

$$u^{(0)}(\mathbf{x}^{n(c,a)}) = \hat{u}^{n(c,a)}. \quad (24)$$

Then, there is no difference between the *sdif* and *mdif* approaches for the first order derivatives, while for the higher order derivatives we have

$$u_{,jk}(\mathbf{x}^c) \approx u^h_{,jk}(\mathbf{x}^c) = \frac{1}{2}\left\{ \sum_{a=1}^{N^c} F_k^{ca} \sum_{\substack{b=1 \\ v=n(c,a)}}^{N^v} F_j^{vb}\hat{u}^{n(v,b)} + \sum_{a=1}^{N^c} F_j^{ca} \sum_{\substack{b=1 \\ v=n(c,a)}}^{N^v} F_k^{vb}\hat{u}^{n(v,b)} \right\}, \tag{25}$$

$$u_{,jkl}(\mathbf{x}^c) \approx u^h_{,jkl}(\mathbf{x}^c) = \underset{jkl}{sym}\left\{ \sum_{a=1}^{N^c} F_l^{ca} \sum_{\substack{b=1 \\ v=n(c,a)}}^{N^v} F_k^{vb} \sum_{\substack{d=1 \\ w=n(v,b)}}^{N^w} F_j^{wd}\hat{u}^{n(w,d)} \right\}, \tag{26}$$

$$u_{,jklm}(\mathbf{x}^c) \approx u^h_{,jklm}(\mathbf{x}^c) = \underset{jklm}{sym}\left\{ \sum_{a=1}^{N^c} F_m^{ca} \sum_{\substack{b=1 \\ v=n(c,a)}}^{N^v} F_l^{vb} \sum_{\substack{d=1 \\ w=n(v,b)}}^{N^w} F_k^{wd} \sum_{\substack{e=1 \\ z=n(w,d)}}^{N^z} F_j^{ze}\hat{u}^{n(z,e)} \right\}, \text{ etc.} \tag{27}$$

where symmetrization is assumed with respect to the indicated indices.
Note that Eqs. (25) - (27) can be rewritten as

$$u^h_{,jk}(\mathbf{x}^c) = \sum_{a=1}^{M^c} F_{jk}^{ca}\hat{u}^{m(c,a)}, \tag{28}$$

$$u^h_{,jkl}(\mathbf{x}^c) = \sum_{a=1}^{N^c} F_l^{ca} \sum_{\substack{b=1 \\ v=n(c,a)}}^{M^v} F_{jk}^{vb}\hat{u}^{m(v,b)} = \sum_{a=1}^{K^c} F_{ljk}^{ca}\hat{u}^{k(c,a)}, \tag{29}$$

$$u^h_{,jklm}(\mathbf{x}^c) = \sum_{a=1}^{N^c} F_m^{ca} \sum_{\substack{b=1 \\ v=n(c,a)}}^{K^v} F_{jkl}^{vb}\hat{u}^{k(v,b)} = \sum_{a=1}^{L^c} F_{jklm}^{ca}\hat{u}^{p(c,a)}, \tag{30}$$

where the global numbers $m(c,a)$ as well as M^c and F_{jk}^{ca}can be obtained from comparison of Eqs. (28) and (25). Similarly from (29) and (26), one can find $k(c,a)$, K^c and F_{ljk}^{ca}, while from (30) and (27), we receive $p(c,a)$, L^c and F_{jklm}^{ca}. For the sake of brevity, we have presented the *modified differentiation* only for MLS-CAN approach.

4.4 Discretized governing equations

Let us summarize various approaches arising in combination of three kinds of formulations for the governing equations (strong formulation – CPDE; local weak formulations: LIE + numerical integration; LIE + analytical integration) with two kinds of approximations (standard MLS approximation; MLS-CAN approximation). Thus, the discussed approaches are shown in Table 1.

Table 1: Review of discussed computational approaches

	strong form	local weak form	
		numerical integr.	analytical integr.
stand MLS	*CPDE + stand MLS*	*LIE(ni) + stand MLS*	*LIE(ai) + stand MLS*
MLS-CAN	*CPDE + (MLS-CAN)*	*LIE(ni) + (MLS-CAN)*	*LIE(ai) + (MLS-CAN)*

Moreover, the higher-order derivatives of the potential field can be treated either by standard differentiation (*sdif*) or by the modified differentiation (*mdif*) approach. Anyway the discretized governing equations can be written compactly as

$$\sum_g K^{cg}\hat{u}^g = -R^c, \quad (c = 1, 2, ..., N_{int}) \tag{31}$$

where N_{int} is the number of interior nodes, the superscripts c and g stand for the global numbers of nodal points. The system matrix K^{cg} and the global numbers of nodes g are to be specified for particular computational approaches as follows:

(i) *CPDE + stand MLS*

$$K^{cg} = \lambda_{ik}(\mathbf{x}^c)\varphi^g_{,ik}(\mathbf{x}^c) + \lambda_{ik,i}(\mathbf{x}^c)\varphi^g_{,k}(\mathbf{x}^c), \quad (g = 1, 2, ..., N_t),\ R^c = w(\mathbf{x}^c) \tag{32}$$

(ii) *CPDE + (MLS-CAN)*

$$K^{cg} = \lambda_{ik}(\mathbf{x}^c)\varphi^g_{,ik}(\mathbf{x}^c) + \lambda_{ik,i}(\mathbf{x}^c)\varphi^g_{,k}(\mathbf{x}^c), \quad (g = n(c,a) \text{ for } a \in \mathscr{M}^c),\ R^c = w(\mathbf{x}^c) \tag{33}$$

If the 2^{nd} order derivative is expressed by *mdif* approach, Eq. (31) can be rewritten as

$$\lambda_{ik}(\mathbf{x}^c)\sum_{a=1}^{M^c} F^{ca}_{ik}\hat{u}^{m(c,a)} + \lambda_{ik,i}(\mathbf{x}^c)\sum_{a=1}^{N^c} F^{ca}_{k}\hat{u}^{n(c,a)} = -R^c. \tag{34}$$

(iii) *LIE(ni) + stand MLS*

$$K^{cg} = \int_{\partial\Omega^c} n_i(\boldsymbol{\eta})\lambda_{ik}(\boldsymbol{\eta})\varphi^g_{,k}(\boldsymbol{\eta})d\Gamma(\boldsymbol{\eta}), \quad (g = 1, 2, ..., N_t),\ R^c = \int_{\Omega^c} w(\mathbf{x})d\Omega(\mathbf{x}) \tag{35}$$

(iv) *LIE(ni) + (MLS-CAN)*

$$K^{cg} = \int\limits_{\partial\Omega^c} n_i(\boldsymbol{\eta})\lambda_{ik}(\boldsymbol{\eta})\varphi^g_{,k}(\boldsymbol{\eta})d\Gamma(\boldsymbol{\eta}), \quad (g \in \{n(q_\eta,a);\ a \in \mathscr{M}^{q_\eta} \text{ for } \forall\boldsymbol{\eta} \in \partial\Omega^c\})$$

$$R^c = \int\limits_{\Omega^c} w(\mathbf{x})d\Omega(\mathbf{x}) \tag{36}$$

If the radius of the sub-domain is sufficiently small ($r_s^c < h^c/2$, where h^c is the minimum distance of any node from $\mathbf{x}^c$), the specification of g is simplified, since $q_\eta = c$ for $\forall\boldsymbol{\eta} \in \partial\Omega^c$ and $g = n(c,a)$ for $a \in \mathscr{M}^c$.

(v) *LIE(ai) + stand MLS*

$$K^{cg} = A^c_k\varphi^g_{,k}(\mathbf{x}^c) + A^c_{kp}\varphi^g_{,kp}(\mathbf{x}^c) + A^c_{kps}\varphi^g_{,kps}(\mathbf{x}^c) + A^c_{kptf}\varphi^g_{,kptf}(\mathbf{x}^c), \quad (g = 1, 2, \ldots, N_t)$$

$$R^c = \frac{1}{\pi(r_s^c)^2}\int\limits_{\Omega^c} w(\mathbf{x})d\Omega(\mathbf{x}) \tag{37}$$

(vi) *LIE(ai) + (MLS-CAN)*

If the higher-order derivatives are expressed by *mdif* approach, Eq. (31) can be rewritten as

$$A^c_k\sum_{a=1}^{N^c} F^{ca}_k\hat{u}^{n(c,a)} + A^c_{kp}\sum_{a=1}^{M^c} F^{ca}_{kp}\hat{u}^{m(c,a)} + A^c_{kps}\sum_{a=1}^{K^c} F^{ca}_{kps}\hat{u}^{k(c,a)} + A^c_{kptf}\sum_{a=1}^{L^c} F^{ca}_{kptf}\hat{u}^{p(c,a)} =$$

$$= -\frac{1}{\pi(r_s^c)^2}\int\limits_{\Omega^c} w(\mathbf{x})d\Omega(\mathbf{x}). \tag{38}$$

Recall that in the case of LIE(ai), the derivatives of the shape functions are required only at the nodal points like in the case of CPDE and in contrast to the LIE(ni) approach. Moreover, in the case of *mdif* –approach, the 1^{st} order derivatives are sufficient.

5 Numerical tests

In order to study the accuracy and convergence of numerical results, we shall consider the example for which exact solution is available. In this paper, we consider a square domain $L \times L$occupied by isotropic medium with exponentially graded heat conduction$\lambda_{ik}(\mathbf{x}) = \delta_{ik}e^{\delta x_2/L}$.

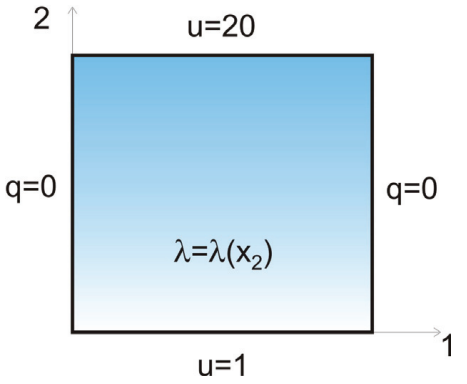

Figure 1: Sketch of the analyzed problem

If constant values of the temperature are prescribed on the bottom $u(0)$ and top $u(L)$ of the square, while the lateral sides are thermally insulated (Fig.1), the exact solution is given as (Sladek et al (2005))

$$u(x) = u(0) + (u(L) - u(0)) \frac{1 - e^{-\delta x_2/L}}{1 - e^{-\delta}},$$
$$q_i(\mathbf{x}) = -\delta_{i2} \lambda(x_2) u_{,2}(x_2) = \frac{\delta}{L} \frac{u(0) - u(L)}{1 - e^{-\delta}} \delta_{i2}. \tag{39}$$

In numerical computations, we have used $\delta = 2$, $u(0) = 1$, $u(L) = 20$. The uniform distribution of nodal points is employed with h being the distance of two neighbour nodes. The % error is evaluated as the average of % errors at all nodal points.

$$\text{error norm } (\%) = 100 \left\{ \sum_{a=1}^{N_t} \Delta u^a \Delta u^a \right\}^{1/2} / \left\{ \sum_{a=1}^{N_t} u^{ex}(\mathbf{x}^a) u^{ex}(\mathbf{x}^a) \right\}^{1/2}, \tag{40}$$

$$\Delta u^a = u^{num}(\mathbf{x}^a) - u^{ex}(\mathbf{x}^a)$$

As regards the computational parameters, we have selected the radius of the support domain (support for the weight functions) $r^a = 3.001 \times h$, the shape parameter $c^a = h$, the radius of circular sub-domains $r_s^a = 0.98 \times h$ in the case of LIE(ni), while $r_s^a = 0.3 \times h$ in the case of LIE(ai). The latter is an optimal value selected from numerical experiments (we have considered also constant values of r_s^a independent on the density of nodes).

First, let us consider the test for accuracy of MLS-approximations for derivatives of the potential field. For this purpose, we present the derivatives along the vertical

line $(L/2, x_2)$ with $x_2 \in [0, L]$. In numerical calculations, we have used 441 nodes. It can be seen (Fig. 2) that the accuracy by *sdif* –approach fails for the 2^{nd} and higher order derivatives, while the *mdif* –approach gives acceptable results at interior nodes except the boundary layer zone. The width of the unacceptable boundary layer zone is increasing with increasing the order of the derivative.

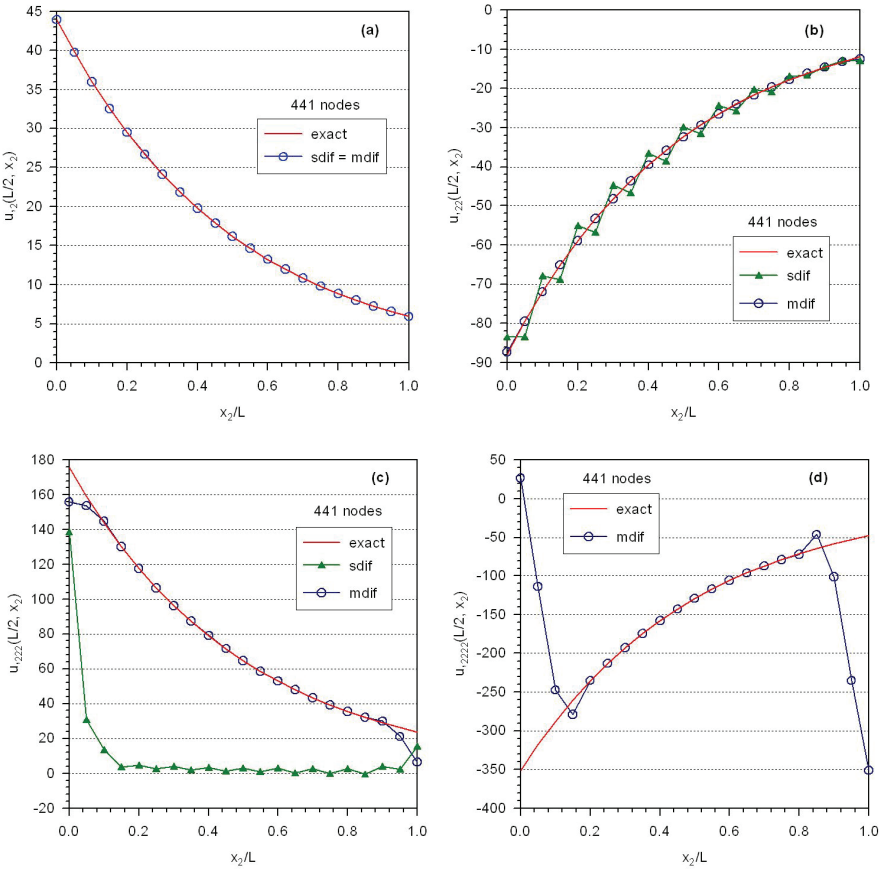

Figure 2: Derivatives of the potential field along the vertical line; (a) 1^{st} order derivative, (b) 2^{nd} order derivative, (c) 3^{rd} order derivative, (d) 4^{th} order derivative

Bearing in mind the superior accuracy for the derivatives of the potential field by *mdif*-approach as compared with the *sdif*-approach, one can expect better accuracy and convergence rate by the *mdif*-approach when applied to implementation of the LIE(ai) technique. This expectation has been confirmed as can be seen from Fig.3, where the accuracy and convergence of numerical results for solution of the

considered b.v.p. by both the LIE(ai)+*sdif* and LIE(ai)+*mdif* have been investigated with decreasing h(increasing the density of nodes). Concluding, we recommend to combine the LIE(ai) computational technique with the *mdif*-approach.

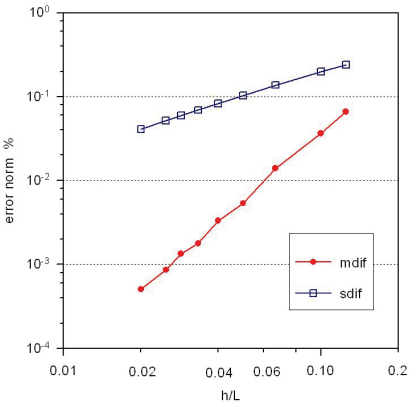

Figure 3: Accuracy and convergence study by LIE(ai)

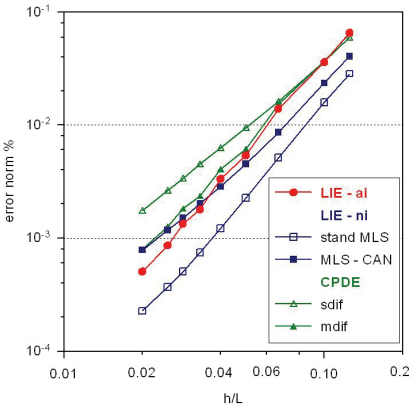

Figure 4: Accuracy and convergence study by various computational techniques

Fig. 4 shows the comparison of accuracies and convergence rates for numerical solution of the considered b.v.p. by using various of the discussed techniques. It can be seen that the best convergence rate is achieved by the LIE(ai) technique, though the best accuracy gives the LIE(ni) implemented by standard MLS-approximation. The last observation can be explained by the fact that only 1^{st} order derivative is required in the LIE(ni) technique and the number of nodes is not truncated in standard MLS-approximation in contrast to the MLS-CAN. Both these facts, however, prolong the computational time.

In Sect. 3, it has been shown that the local weak form given by LIE(ai) is converted to the strong form in the limit $r_s^c \to 0$ (as the radius of the local sub-domain approaches zero). Now, Fig. 5 illustrates the confirmation of this statement also by numerical results.

For assessment of the efficiency of particular computational techniques, we shall utilize the computational times t_{sm} - time needed for creation of the matrix of the system of discretized equations, t_{sol} - time needed for solution of that system, and t_{tot}- total computational time. From Fig. 6, we can see that the standard differentiation approach (*sdif*) yields longer t_{sm} than *mdif* when combined with the LIE(ai) technique. Thus, in view of this result and the results on Fig. 3, the LIE(ai) + *mdif* is superior.

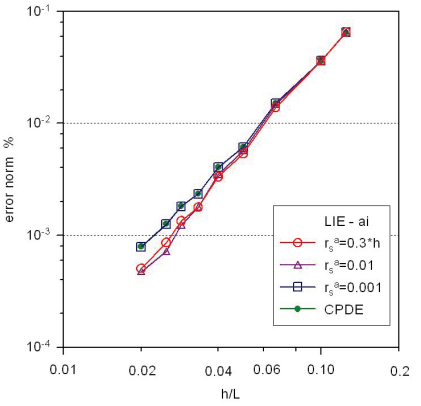

Figure 5: Investigation of numerical limit $r_s^c \to 0$ in accuracy study by LIE(ai)

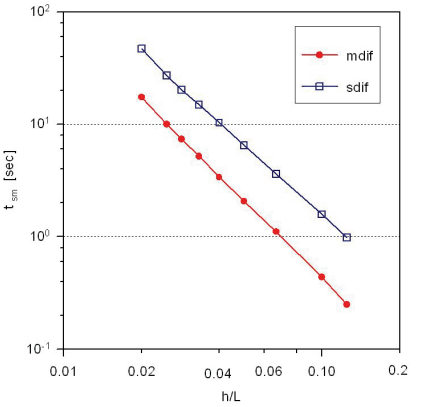

Figure 6: Computational times for creation of the system matrix in LIE(ai) technique

From comparison of t_{sm} for various techniques, we see that there is small difference between the LIE(ai) and CPDE but significantly higher times t_{sm} are needed in the case of LIE(ni). The utilization of the MLS-CAN approximation can produce great savings in t_{sm} as compared with standard MLS especially in the case dense distributions of nodes.

Fig. 8 confirms the expectation that the differences in t_{sol} by various techniques for creation of the discretized equations are negligible.

Since the t_{sol} is almost independent on the employed computational technique for creation of the system matrix, the savings in t_{sm} should be visible also in the total computational time t_{tot}. This fact is illustrated in Fig. 9.

In order to assess the role of solver, we have used for comparison two standard solvers GELG and DGESV. Fig. 10 shows that the benefit of faster solver is worthful for problems with huge amount of d.o.f. Note that the LIE(ni) is less sensitive to the employed solver especially if the standard MLS is used for the approximation of field variables.

6 Conclusions

The meshless approximations prolong the computational time needed for creation of system matrices especially in weak formulations. We propose to diminish this handicap in two ways:

(A) by introducing *CAN-concept in the MLS-approximation*

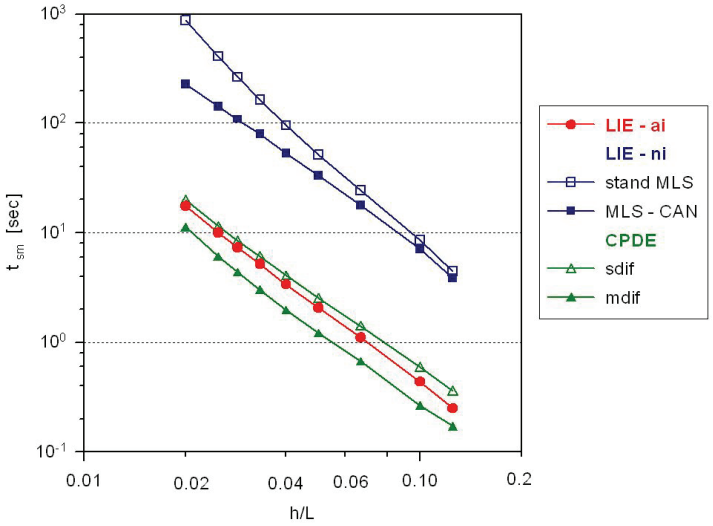

Figure 7: Comparison of t_{sm} by various computational techniques for various densities of distribution of nodal points

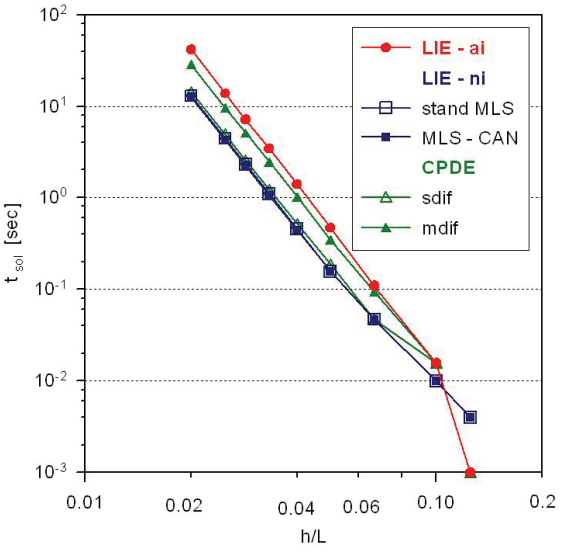

Figure 8: Dependence of t_{sol} on the density of nodes with using the Lapack solver DGESV

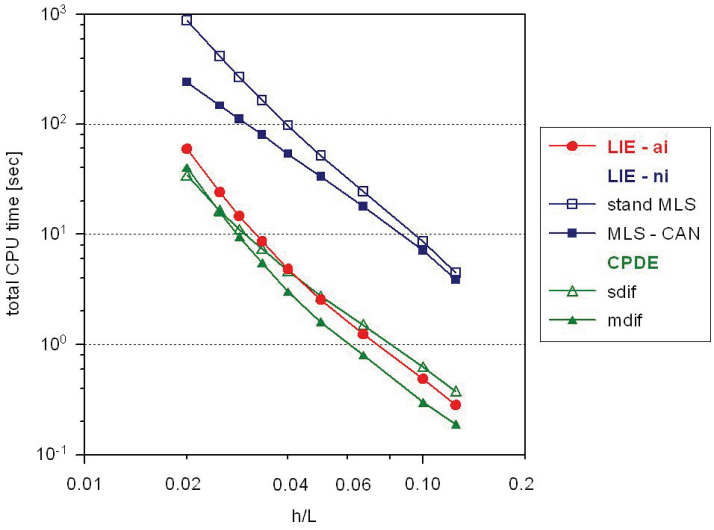

Figure 9: Dependence of t_{tot} on the density of nodes for various computational techniques

(B) by *combining meshless approximations with analytical integrations*.

(A) The method based on the LIE+numerical integration involves only the 1^{st} order derivatives. This method results into the best accuracy but also into the worst computational economy. The MLS-CAN approximation *does not introduce higher order derivatives*, while *the CPU time is decreased with keeping the accuracy to be still reasonable*.

(B) The analytical integration assumes Taylor series expansion of the shape functions what results in appearance of higher order derivatives of the shape functions.

The reasonable *accuracy of higher-order derivatives* of shape functions can be achieved by the proposed *modified differentiation* based on the representation of such derivatives in terms of the first-order derivatives.

The are proposed two approaches based on:

*LIE+analytical integration+modified differentia*tion

CPDE+modified differentiation

resulting in *significant savings of computational time needed for creation of system matrix*. Moreover, there are achieved *higher convergence rate* and *better accuracy* than by methods utilizing standard differentiation of the shape functions

The effective utilization of savings achieved in t_{sm} requires *fast solvers* especially

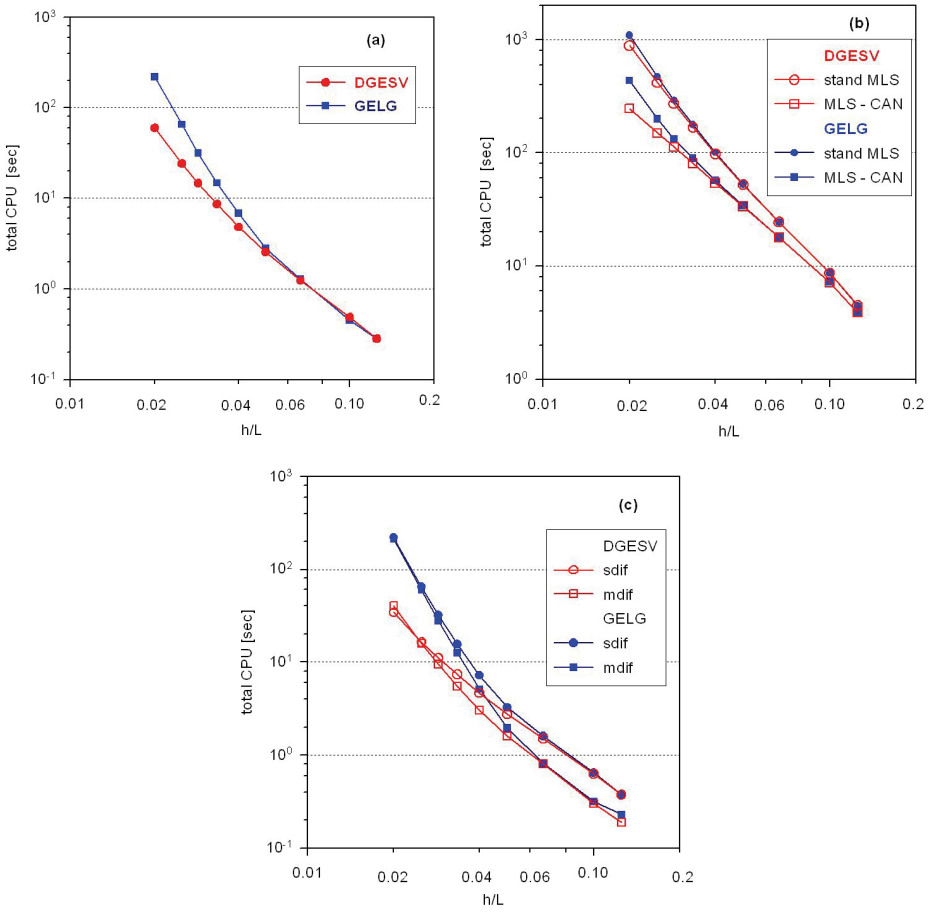

Figure 10: Influence of employed solver on t_{tot} for: (a) LIE(ai), (b) LIE(ni), (c) CPDE

in problems with huge amount of unknowns.

References

Atluri, S.N.; Han, Z.D.; Shen, S. (2003): Meshless local Petrov-Galerkin (MLPG) approaches for solving the weakly-singular traction & displacement boundary integral equations. *CMES: Computer Modeling in Engineering & Sciences*, 4: 507-516.

Atluri, S.N. (2004): *The Meshless Method, (MLPG) For Domain & BIE Discretizations*, Tech Science Press, Forsyth.

Lancaster, P.; Salkauskas, K. (1981): Surfaces generated by moving least square methods. *Math. Comput*., 37: 141-158.

Liu, G.R. (2003): Mesh free methods, Moving beyond the finite element method, CRC Press, Boca Raton.

Sladek, V.; Sladek, J.; Tanaka, M.; Zhang, Ch. (2005): Local integral equation method for potential problems in functionally graded anisotropic materials. *Eng. Anal. Bound. Elements*, 29: 829-843.

Sladek, V.; Sladek, J.; Zhang, Ch. (2008a): Computation of stresses in non-homogeneous elastic solids by local integral equation method: a comparative study. *Computational Mechanics*, 41: 827-845.

Sladek, V.; Sladek, J.; Zhang, Ch. (2008b): Local integral equation formulation for axially symmetric problems involving elastic FGM. *Eng. Anal. Bound. Elem*., 32: 1012-1024.

Sladek, V.; Sladek, J.; Zhang, Ch. (2008c): Analytical integrations in meshless implementations of local integral equations. In: B.A. Schrefler, U. Perego (eds.) *Proc. 8th World Congress on Computational Mechanics WCCM8*, Int. Center for Numerical Methods in Engn. (CIMNE): Barcelona, CD –ROM, ISBN 978-84-96736-55-9.

Sladek, V.; Sladek, J.; Zhang, Ch. (2009): Meshless implementations of local integral equations. In: Brebbia, C.A. (ed) *Mesh reduction methods*. WIT Press, Southampton, 71–82.

Sladek, V.; Sladek, J. (2010): Local integral equations implemented by MLS-approximation and analytical integrations. *Eng. Anal. Bound. Elem*., doi10.1016j.enganabound.2010.03.015.

Wen, P.H.; Aliabadi, M.H. (2008): An improved meshless collocation method for elastostatic and elastodynamic problems. *Commun. Numer. Meth. Engng*., 24: 635-651.

Wrobel, L.C. (2002): *The Boundary Element Method, Vol1: Applications in Thermo-Fluids and Acoustics*, John Wiley & Sons, Chichester.